To be published in
IEEE Trans. Nucl. Sci.

BNL-23453

Presented at IEEE Nuclear Science
Symposium, 19-21 October 1977,
Sheraton Palace Hotel, San Francisco

AVALANCHE LOCALIZATION AND ITS EFFECTS IN PROPORTIONAL COUNTERS*

J. Fischer, H. Okuno† and A. H. Walenta‡

Brookhaven National Laboratory
Upton, New York 11973

November 1977

*Research carried out under the auspices of the Energy Research and Development Administration: Contract No. EY-76-C-02-0016.

†On leave from Institute for Nuclear Study, University of Tokyo, Tanashi, Tokyo, Japan.

‡On leave from University of Heidelberg, Heidelberg, Germany.

DISCLAIMER

AVALANCHE LOCALIZATION AND ITS EFFECTS IN PROPORTIONAL COUNTERS*

J. Fischer, H. Okuno† and A. H. Walenta‡

Brookhaven National Laboratory
Upton, New York 11973

Abstract

Avalanche development around the anode wire in a gas proportional counter is investigated. In the region of proportional gas amplification, the avalanche is found to be well localized on one side of the anode wire, where the electrons arrive along the field lines from the point of primary ionization. Induced signals on electrodes surrounding the anode wire are used to measure the azimuthal position of the avalanche on the anode wire. Practical applications of the phenomena such as left-right assignment in drift chambers and measurement of the angular direction of the primary ionization electrons drifting towards the anode wire are discussed.

Introduction

Early studies on the spatial development of the avalanche relative to the anode wire were concentrated on the radial development,[1] whereas in modern application of multiwire proportional chambers (MWPC) and multiwire drift chambers (MWDC), knowledge of the azimuthal or angular extent of the avalanche around the anode wire becomes important not only for a more precise understanding of the gas multiplication process but also for improvement of particle position measurements by adding another information, the direction of electron drift to the anode wire.

At the beginning of MWPC development, observation of induced signals on adjacent wires led to the assumption that the avalanche surrounds the anode wire uniformly at least at high gas gain.[2] However, more recent studies of induced signals have indicated some asymmetry in the avalanche development around the anode wire.[3-7]

In this paper, we report on an investigation on the question whether the avalanche is confined to one side of the anode wire or spreads around the anode wire by measuring positive ions of the avalanche. Indeed, it was found that the avalanche is well confined to one side of the anode wire in the proportional region of gas amplification.[xx] Since the avalanche is localized, induced signals on electrodes surrounding the anode wire contain some information on the azimuthal position of the avalanche. Therefore we studied the formation of induced signals due to the localized avalanche in detail. Applications of the avalanche localization phenomena to MWPC's and MWDC's are also discussed.

Avalanche Localization

The first method which has been applied to study the localization of the avalanche is to measure positive ion signals at potential wires in a MWDC.[3] The principle of the method is shown in Fig. 1. A collimated source is placed near the potential wire PW. Electrons liberated by the ionization drift toward the anode wire along the field lines and are multiplied in the stong field near the anode wire. If electrons do not spread around the anode wire through these processes, positive ions created in the avalanche are also localized and trace back the same field lines in opposite direction as the electrons drifted. An arrival of positive ions in the strong field around the potential wire PW gives induced signal on PW. If the avalanche surrounds the anode wire, positive ions will also drift to the potential wire $\overline{PW}$ on the side of the anode wire where no primary ionization is produced.

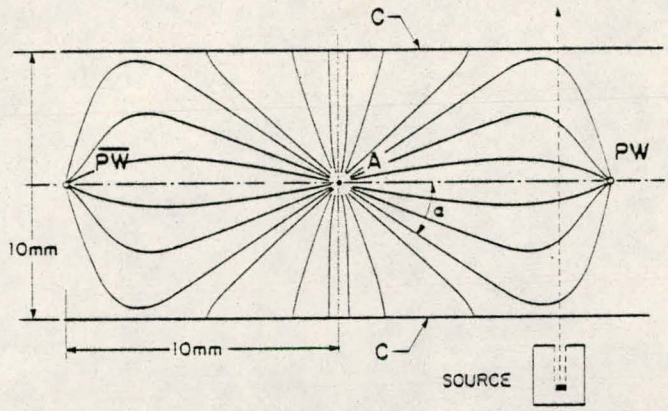

Figure 1

Field line configuration in a drift chamber. A: anode wire (30 μm dia., 1.75 kV), PW and $\overline{PW}$: potential wires (100 μm dia., - 0.2 kV) and C: cathode planes (ground).

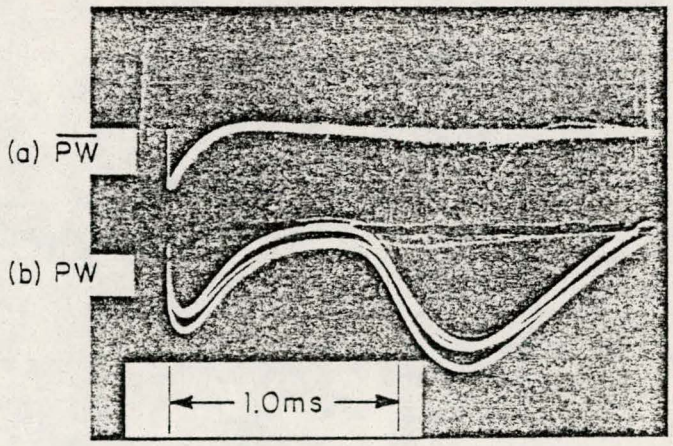

Figure 2

Signals on potential wires, $\overline{PW}$ and PW. Amplifier differentiation time constant: t = 100 μs. Reversed polarity.

Typical signals on PW and $\overline{PW}$ are shown in Fig. 2.

*This research was supported by the U. S. Department of Energy: Contract No. EY-76-C-02-0016.

†On leave from Institute for Nuclear Study, University of Tokyo, Tanashi, Tokyo, Japan.

‡On leave from University of Heidelberg, Heidelberg, Germany.

xxDetails are given in Ref. 8.

A large signal of positive ions is seen on PW in addition to the immediate induced signal at the beginning, but a signal of positive ions is not visible on $\overline{PW}$. For higher gas gain, however, it becomes visible and the ratio of these positive ion signals $R = A(\overline{PW})/A(PW)$ is used to determine the azimuthal spread of the avalanche around the anode wire.

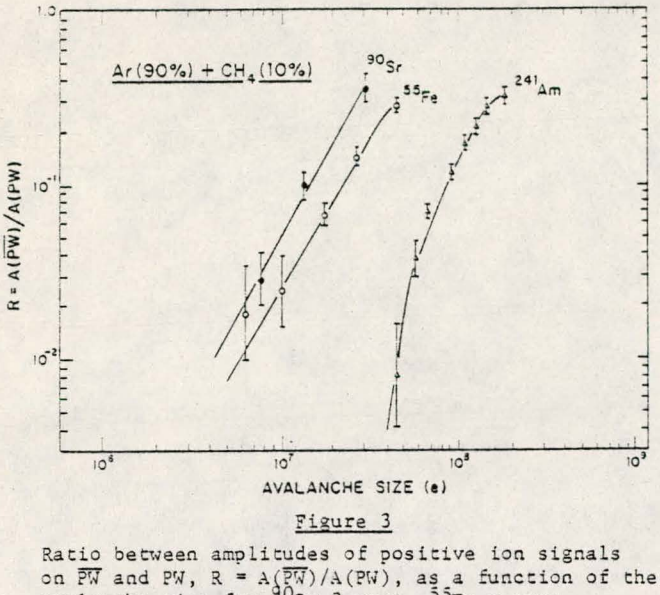

Figure 3

Ratio between amplitudes of positive ion signals on $\overline{PW}$ and PW, $R = A(\overline{PW})/A(PW)$, as a function of the avalanche size for ^{90}Sr β-rays, ^{55}Fe x-rays, and ^{241}Am α-rays. Gas: $Ar(90\%)+CH_4(10\%)$.

The results of R for $Ar(90\%)/CH_4(10\%)$ are shown in Fig. 3 as a function of the avalanche size Q_A which is expressed as an equivalent number of electron charges collected on the anode in 1 μs. In the proportional region, $Q_A \leq 5 \times 10^6 e$ for ^{90}Sr β-rays and ^{55}Fe x-rays, it can be concluded that the avalanche is well confined to one side of the anode wire. By increasing the voltage, one leaves the truly proportional region which is characterized by a first Townsend process. Then two effects become noticeable, the gas multiplication starts to be aided by photon propagation and the development of space charge reduces the effective field near the anode wire which saturates the gas amplification. In this semi-proportional region, the localization phenomena depend on such factors as the voltage, the gas mixture and the density of primary ionization. In general, the photon process tends to spread the avalanche around the anode wire since the photon does not follow the field lines. The effect of photon quenching can be seen, for example, in CH_4 where the spread is much suppressed compared to $Ar(90\%)/CH_4(10\%)$ at the same gain. For ^{241}Am α-rays, R is less than 1% up to $Q_A = 5 \times 10^7 e$, where the effect of photon process is still small because of lower electric field and therefore lower gas gain.

The second method used to obtain information of the avalanche localization was to measure the center of gravity of induced charges on the cathode in a MWPC with a high precision delay line placed orthogonal to the anode wire.[6,8] If the avalanche is localized to one side of the anode wire as described above, the measurement of the center of gravity of induced charges relative to the anode wire gives us an approximate indication of the radial distance of the avalanche from the anode wire. Figure 4 shows a typical measurement for ^{55}Fe x-rays in $Ar(80\%)/CO_2(20\%)$, where two distinct locations of the position spectra correspond to avalanches which started either from the left or the right side of the anode wire. Observed distances between the two peaks, ΔX, are shown in Fig. 5 for $Ar(90\%)/CH_4(10\%)$

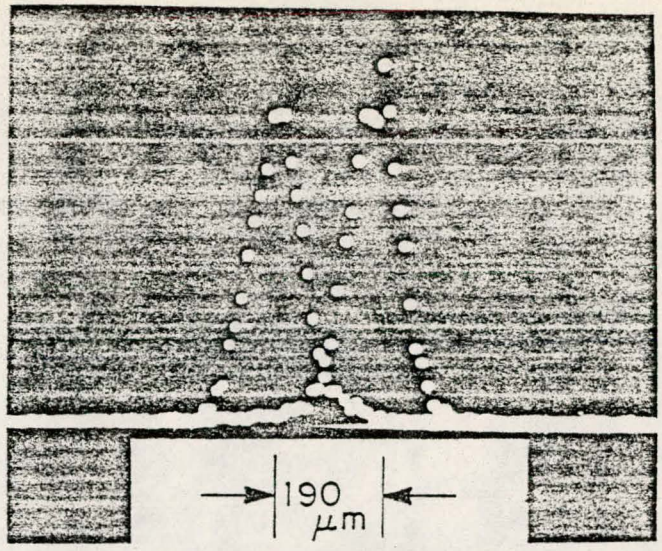

Figure 4

Position spectra of avalanches measured with the ^{55}Fe x-ray source 2.5 mm on either side of the anode wire, gas: $Ar(80\%)+CO_2(20\%)$, HV: 2.3 kV and spatial resolution: $\sim$ 85 μm FWHM. Distance between peaks: 190 μm.

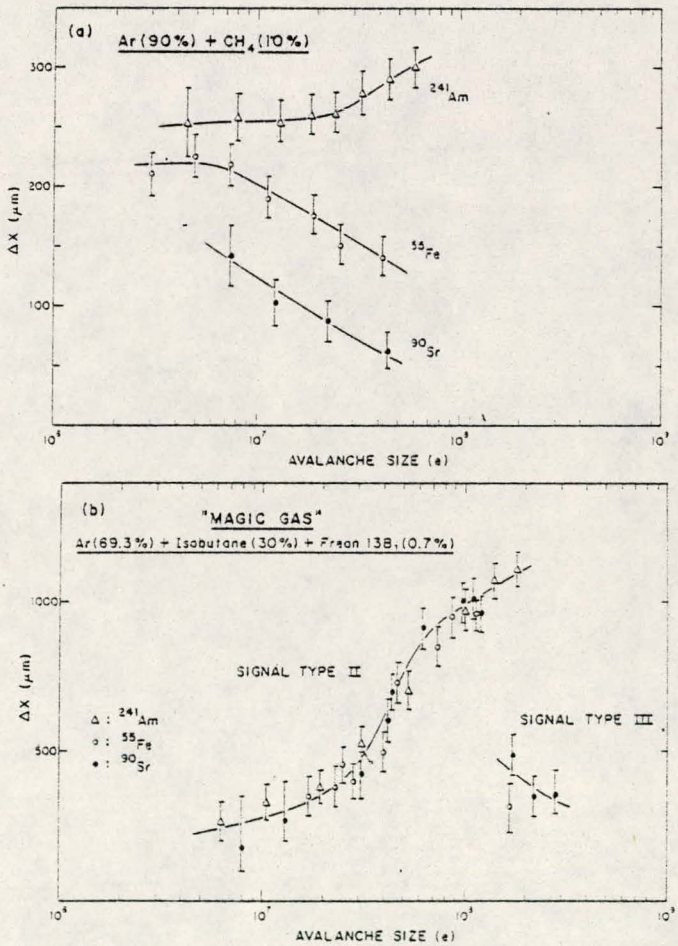

Figure 5

Measured distance, ΔX, between left and right avalanches as a function of the avalanche size for ^{90}Sr β-rays, ^{55}Fe x-rays and ^{241}Am α-rays. (a) Gas: $Ar(90\%)+CH_4(10\%)$ and (b) "magic gas" $Ar(69.3\%)$ + Isobutane (30%) + Freon 13B1 (0.7%).

and "magic gas", Ar(69.3%)/Isobutane (30%)/Freon 13B1 (0.7%). At an avalanche size of less than $Q_A \leq 5 \times 10^6$e, ΔX = 200 ~ 250 μm for all gas mixtures. By increasing the applied voltage, ΔX decreases for ^{90}Sr β-rays and for ^{55}Fe x-rays in Ar(90%)/CH_4(10%) indicating that the avalanche spreads around the anode wire, but for ^{241}Am ΔX actually increases which indicates a still localized avalanche. This is consistent with the positive ion measurement.

However, for magic gas, a completely different behavior was observed. In the "magic mode" or amplitude saturating region, ΔX increases up to 1 mm and then it suddenly decreases. The measurement of positive ions also showed the same behavior that the avalanche only partially surrounds the anode wire under these conditions.

The relation between the real position of the avalanche and the observed value of ΔX is complicated because the distribution of the image charge due to the azimuthally localized avalanche on the anode wire is distorted on the cathode by the existence of the anode wire near the avalanche. A study with an electrostatic model showed that,[8] ΔX = 1 mm between observed peaks corresponds to an actual distance of about 600 μm, or a distance of 300 μm to the anode wire. Our delay line method is sensitive to the mean value of the induced charges in about 10 ns. When we assume that positive ions move only in one direction from the anode wire then they would be 30-40 μm away in 10 ns and this corresponds to $\Delta X \simeq$ 200 μm, which is in agreement with the observation in the proportional region. For magic gas, however the center of gravity of the avalanche in 10 ns is found to be relatively far from the anode wire. This is also indicated by the observation of the fast rise time of the anode signal due to the electron contribution to the signal formation.

An interpretation of the "magic mode" assuming the avalanche to start and stop multiplication at a large distance (~ 300 μm) from the anode wire would be difficult because the field strength at 300 μm from the wire is too low to get enough gas amplification. However, when we assume that the photon process sets in and that the mean free path of the photon is relatively short, the avalanche may develop from the anode wire outwardly, because although the field strength between the anode wire and the avalanche becomes lower, the field strength outside of the avalanche increases due to the strong space charge effect.

Induced Signals

If the avalanche is localized rather than spread around the wire, the relationship of the induced charge on surrounding electrodes is a measure of the position of the avalanche not only along the anode wire but also the azimuthal position around the anode wire.

To study induced signals in more detail, and approximate a configuration of practical use, we used a square chamber shown in Fig. 6. Induced signals are read out from cathode strips along each wall. Typical signals on cathodes U and D are shown in Fig. 7, when the ^{55}Fe x-rays are injected on the side of cathode U. The differentiation time constant of the preamplifier was 2.5 ms, long enough to study the whole time development of the induced charge. Although they have the same polarity, the signal shape is quite different.

The time development of induced charges on cathode strips U and D is studied with an electrostatic model, assuming a point charge moving in one direction from the anode wire. In general, the charge induced on an electrode due to the point charge q is given by*

$$Q_i = q \cdot f_i(x,y) \quad , \qquad (1)$$

where $f_i(x,y)$ is a weighting function depending, in a given electrode system, only on a location (x,y) of q. Following Green's reciprocal theorem, $f_i(x,y)$ is expressed as

$$f_i(x,y) = \frac{V'(x,y)}{V_o'} \quad , \qquad (2)$$

where $V'(x,y)$ is the potential at point (x,y) when the potential V_o' is applied on the electrode i where the induced charge will be measured and all other electrodes are kept at zero potential.

A convenient way to obtain $f_i(x,y)$ is by the use of a model of resistive paper where electrodes are represented by conductive paint. Figure 8 shows the equipotential line of $f_U(x,y)$ for cathode U of the square chamber obtained with this method.

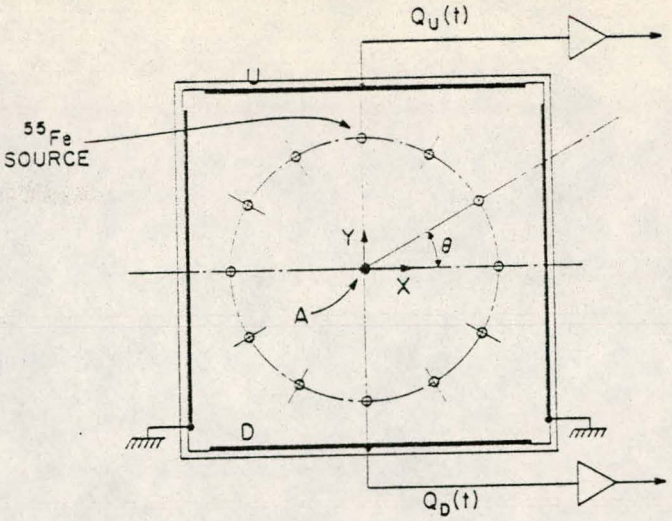

Figure 6

Square chamber 25.4 mm x 25.4 mm x 90 mm. A: anode wire (25 μm dia.), U and D: cathode strips for induced signals. Collimated x-rays are injected parallel to the anode wire.

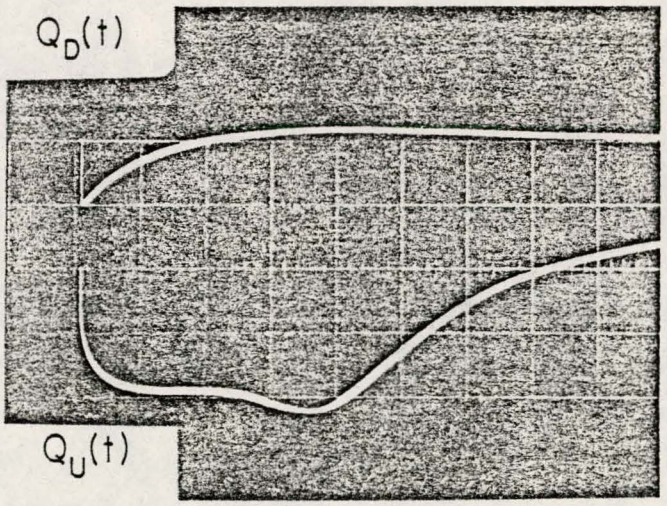

Figure 7

Induced signals on cathode strips U and D, when the ^{55}Fe x-rays are injected on the side of cathode strip U. Amplifier differentiation time constant: τ = 2.5 ms.

*A more detailed description is given in Ref. 9.

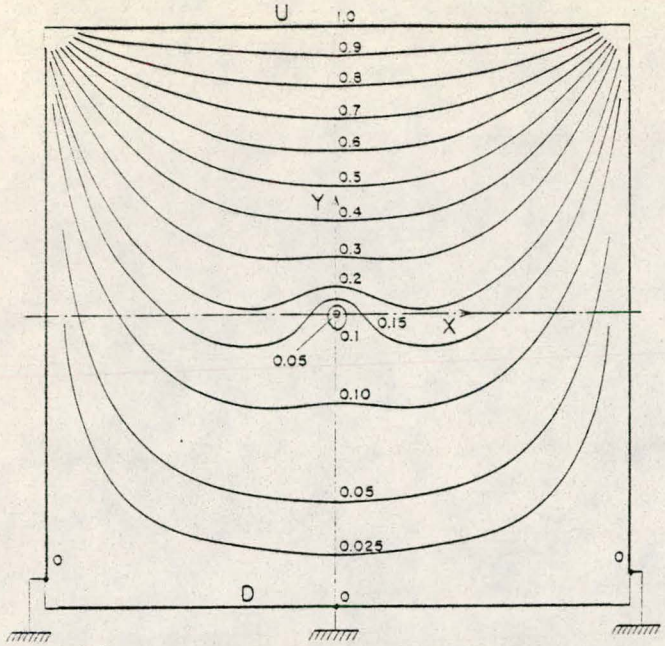

Figure 8

Equipotential lines for the determination of the weighting function $f_U(x,y)$ of the upper cathode strip U.

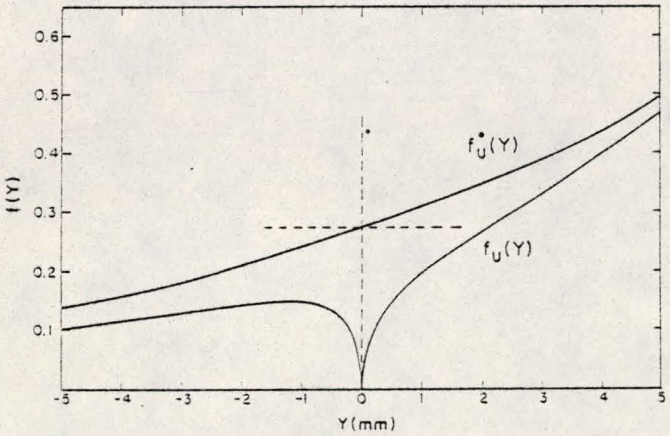

Figure 9

Weighting functions along the Y-axis for the upper cathode strip U. f_U: with the anode wire grounded. f_U^o : without the anode wire.

In Fig. 9, $f_U(x,y)$ along the Y-axis is shown, where a sharp dip can be seen at the point of the anode wire. The weighting function without the anode wire is also shown for comparison.

As the point charge q moves away from the anode wire in one direction, the time development of induced charges is obtained by expressing the position of q as a function of time t in eq. 1. The electric field for the movement of positive ions near the anode wire is approximated by the field of a cylindrical condenser with inner radius r_i and outer radius r_o, the position of positive ions at time t is given by

$$r(t) = \left(\frac{2\mu^+ V_o}{\ln(r_o/r_i)}\, t + r_i^2 \right)^{\frac{1}{2}} \quad , \qquad (3)$$

where μ^+ is the mobility of positive ions and V_o is the applied voltage on the anode. By using $\mu^+ = 1.7$ cm^2/kV·ms for CH_4^+ ions in Ar(90%)/CH_4(10%), $Q_U(t)$ and $Q_D(t)$ are calculated for positive ions moving along the Y-axis from the anode toward the cathode U, and are shown in Fig. 10.

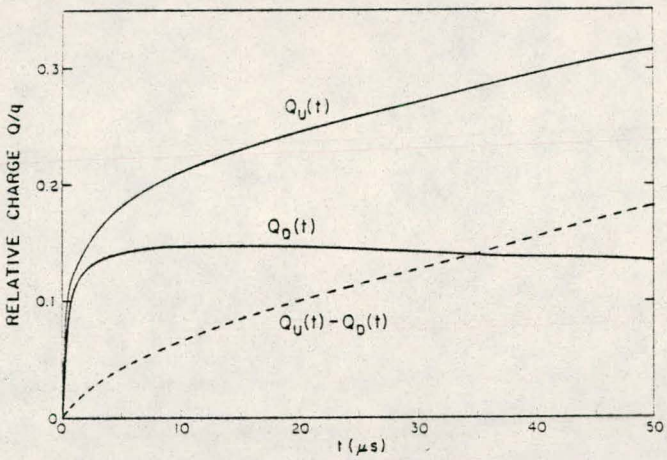

Figure 10

Time development of the induced charges on cathode strips U and D, normalized with the amount of the moving charge. The dotted line shows their difference.

There is no big difference in amplitude at the beginning and, as positive ions leave the anode, $Q_D(t)$ starts to decrease, however, $Q_U(t)$ continues to increase. Thus the signal shape observed in the real chamber is well expressed with this method.

Azimuthal Position of the Avalanche

As the induced signals, especially the difference signal $Q_U(t) - Q_D(t)$, contain information on the azimuthal position of the avalanche, we extend the analysis into two dimensions. Because of the radial field around the anode wire, it is convenient to use the (r,θ) polar coordinates. Using the relation $f_U(r,\theta + \pi) = f_D(r,\theta)$, the difference of induced signals is given by

$$Q_U(t) - Q_D(t) = q \cdot \left\{ f_U(r,\theta) - f_U(r,\theta + \pi) \right\} \quad . \qquad (4)$$

Since the diameter of the anode wire is small compared to the distance between the anode wire and the cathodes, it can be treated as a line charge with an infinitesimal diameter.* Then $f_U(r,\theta)$ can be considered to be built up by the weighting function $f_U^o(r,\theta)$ for an electrode arrangement without the anode wire and the superposition of a very steep weighting function of the anode wire. As the latter is symmetric around the anode wire, eq. 4 can be rewritten in good approximation as

$$Q_U(t) - Q_D(t) \approx q \cdot \left\{ f_U^o(r,\theta) - f_U^o(r,\theta + \pi) \right\} \quad . \qquad (5)$$

$f_U^o(r,\theta)$ near the anode wire is approximated as

$$f_U^o(r,\theta) \approx \left. \frac{\partial f_U^o}{\partial r} \right|_{\substack{r = o \\ \theta = \pi/2}} \cdot r \cdot \sin\theta \quad . \qquad (6)$$

*More exact treatment of the anode wire of radius r_i would include the effect of the dipole charge on the anode wire. But the angular dependence of the difference signal remains unchanged.

Finally, by the use of eq. 3, we get

$$Q_U(t) - Q_D(t) \approx 2q \cdot \left.\frac{\partial f_U^o}{\partial r}\right|_{\substack{r=o \\ \theta=\pi/2}} \cdot \left(\frac{2\mu^+ V_o}{\ln(r_o/r_i)}\, t + r_i^2\right)^{\frac{1}{2}} \cdot \sin\theta \quad (7)$$

This clearly explains the characteristic features of the difference signal. The amplitude of the difference signal is proportional to the steepness of the weighting function without the anode wire and varies as $\sin\theta$. The time development is in good approximation proportional to $\sqrt{t}$.

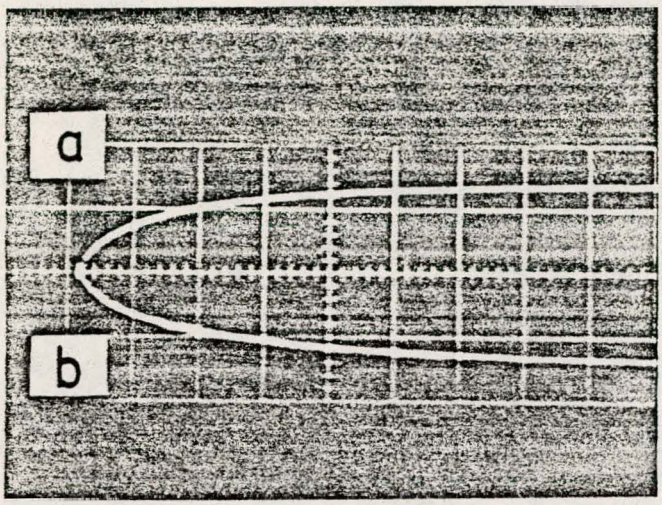

Figure 11

Pulse shape of difference signals, $Q_U(t) - Q_D(t)$. Differentiation time constant $\tau \cong 25$ μs. (a) $\theta = 90°$ and (b) $\theta = 270°$.

Typical pulse shapes of the difference signal are shown in Fig. 11 for two angular positions of the collimated ^{55}Fe x-rays; $\theta = 90°$ and $\theta = 270°$. Pulse height spectra of the difference signal normalized with the anode amplitude are shown in Fig. 12, where source positions are (a) $\theta = 30°$, (b) $\theta = 60°$ and (c) $\theta = 90°$, and $t = 5$ μs. Angular dependence of the amplitude of the difference signal is shown in Fig. 13, which shows a complete agreement with the expected $\sin\theta$ variation. The resolution of the angle measurement is $\pm 5°$ (FWHM) at $\theta = 30°$ which is limited here by the source collimation. These results show that the azimuthal position of the avalanche around the anode wire can be measured precisely with induced signals on a set of electrodes around the anode wire.

Conclusion

Our study showed that, in the proportional region of gas amplification, the avalanche is well localized on one side of the anode wire. By increasing the applied voltage, the avalanche starts to spread around the anode wire to some extent by the photon process.

Investigation of induced signals from the localized avalanche shows that the information on the azimuthal angular position of the avalanche can be extracted from the measurement of induced signals on a set of electrodes.

As the avalanche is formed by electrons which drifted toward the anode wire along known DC field lines, the measurement of the azimuthal position of the avalanche determines the particular drift path of electrons from each point of primary ionization. This

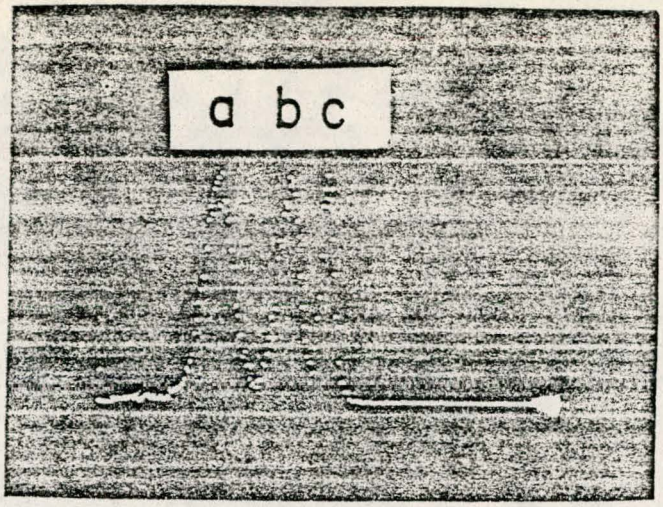

Figure 12

Pulse height spectra of the difference signals, $Q_U(t) - Q_D(t)$, normalized with the amount of anode charge. Angular positions of ^{55}Fe x-ray source are (a) $\theta = 30°$, (b) $\theta = 60°$ and (c) $\theta = 90°$. Gas: Ar(90%)+CH_4(10%), HV: 1.7 kV, signal gate time: 5 μs.

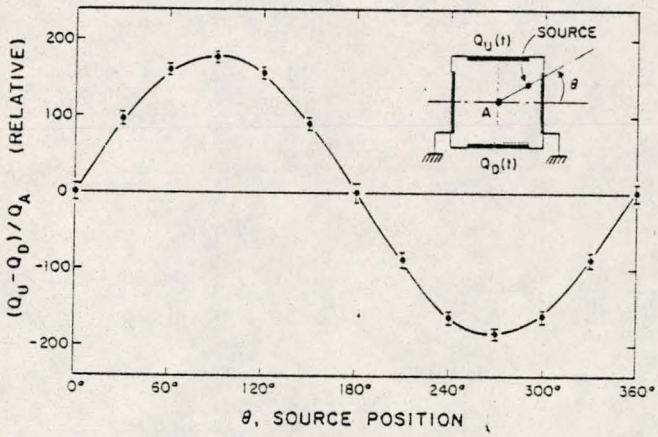

Figure 13

Angular dependence of the amplitude of the difference signal for ^{55}Fe x-rays.

is very useful for practical applications. The read-out of induced signals on potential wires or neighboring cathodes in MWDC's make it possible to solve the left-right ambiguity with high precision.[9] It is also useful for the half-gap discrimination in MWPC's for x-ray imaging.[7] As demonstrated in this paper, the precise measurement of the angular position of the avalanche makes it possible to determine the azimuthal angle of the primary ionization point in a single counter. This combined with measurements of the electron drift time and the avalanche position along the anode wire, could locate three dimensional coordinates of the interaction point for, e.g., x-rays and neutrons.

Acknowledgements

The authors express their appreciation to Dr. V. Radeka and Prof. E. Gatti for many helpful discussions.

NOTE: A related study of the avalanche localization phenomena in MWPC is also reported by G. Charpak et al at this conference.

References

1. S. A. Korff; Electron and Nuclear Counters (Van Nostrand, New York 1946).
2. G. Charpak, D. Rahm, and H. Steiner; Nucl. Instr. and Meth. 62 (1970) 13, G. Charpak; Ann. Rev. Nucl. Sci. 20 (1970) 195.
3. A. H. Walenta, J. Heintze, and B. Schürlein; Nucl. Instr. and Meth. 92 (1971) 373.
4. G. Charpak and F. Sauli; CERN 73-4, Feb. 1973.
5. H. E. Kraft; Diplomarbeit, Heidelberg, 1974.
6. H. Okuno, R. L. Chase, J. Fischer and A. H. Walenta; IEEE Trans. Nucl. Sci., NS-24 (1977) 213.
7. C. J. Borkowski and M. K. Kopp; IEEE Trans. Nucl. Sci., NS-24 (1977) 287.
8. J. Fischer, H. Okuno and A. H. Walenta; BNL 23163 (1977), to be published in Nucl. Instr. and Meth.
9. A. H. Walenta; BNL 23162 (1977), to be published in Nucl. Instr. and Meth.